State-of-the-art of elevation extraction from satellite SAR data

Thierry Toutin* , Laurence Gray
Canada Centre for Remote Sensing
588 Booth Street, Ottawa, Canada K1A 0Y7

Abstract

Relative or absolute elevation extraction from satellite radar data has been an active research topic for more than 20 years. Various investigations have been made on different methods depending on the predominant "fashion" and data availability, leading each time to new developments to improve the capability and the applicability of each method. The paper presents an update of the state-of-the-art of elevation extraction from satellite SAR data. The performance and limitations of four different methods (clinometry, stereoscopy, interferometry and polarimetry) are reviewed, as well as their applicability to different satellite SAR sensors. Their advantages and disadvantages are also analysed and how they are addressed during the data processing. Finally, concluding remarks look at the complementarity aspects of each method to make the best use of the existing and future radar data for elevation extraction.

Keywords: DEM; satellite SAR; clinometry; shape-from-shading; stereoscopy; interferometry; polarimetry

1. Introduction

With the advent of instruments that produce images from electromagnetic radiation beyond wavelengths to which the human eye and cameras are responsive, human "vision and perception" has been greatly extended. Remote sensing has evolved into an important

* Corresponding author. E-mail: thierry.toutin@ccrs.nrcan.gc.ca

supplement to ground observations and aerial images in the study of terrain features, such as ground elevation. Digital elevation models (DEMs) are currently one of the most important data used for geo-spatial analysis. Unfortunately, DEMs of sufficient point density are still not available for many parts of the Earth, and when available they do not always have sufficient accuracy. Since a DEM enables easy derivation of subsequent information for various applications, elevation modeling has become an important part of the international research and development (R&D) programs related to geo-spatial data.

Due to high spatial resolution of civilian satellite synthetic aperture radar (SAR) sensors since the 1980s with the Shuttle Imaging Radar (SIR), a large number of researchers around the world have investigated the elevation modeling and the production of DEMs. Recent discussions on different aspects of radar for radargrammetry and for cartography can be found in Leberl (1990) and Polidori (1997), respectively. Furthermore, the recent research in computer vision to model human vision has led to the advent of new alternatives applied to satellite imagery.

Since the elevation extraction is an active R&D topic, the objective of the paper is to update the previous reviews, mainly with the launch of the Canadian RADARSAT in 1995 and the research studies related to its different SAR imaging capabilities (Fig. 1). Four different methods (Fig. 2) (clinometry, stereoscopy, interferometry and polarimetry) to extract relative or absolute elevation are then reviewed with their advantages and disadvantages. Their applicability to the different satellite SAR data is also presented. Finally, some concluding remarks on these methods and their complementarity, and prospects for the future with the next generation of satellites are drawn.

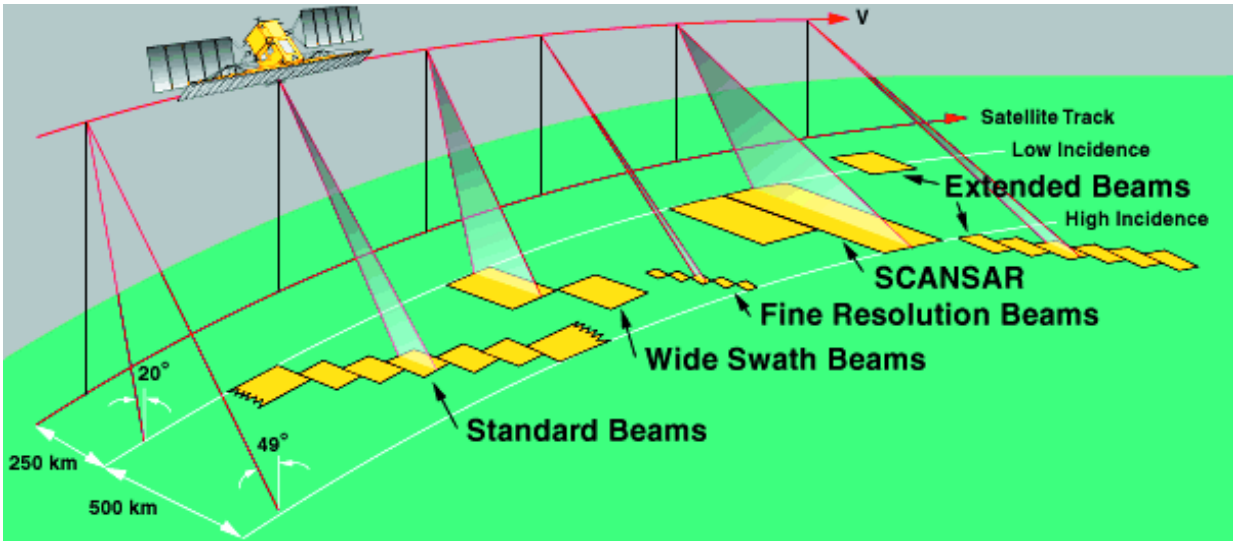

Fig. 1. Operating modes of RADARSAT-SAR (C-band, HH polarisation).

2. Clinometry

Shade, shadows and occluded areas are familiar phenomena, which can help judge size and shape of objects by providing an impression of convexity and concavity. They are particularly helpful if the objects are very small or lack tonal contrast with their surroundings. These familiar phenomena are used to extract relative elevations of specific targets or terrain elevations from a single image. However, shadowing and shading are sometimes confused.

2.1. Shadow / occluded areas

Shadow only provides localised cues (along special contours) of shape, although the shadow of a curved surface cast on another curved surface is very difficult to interpret. The shadow areas then occur when the ground surface is not illuminated by the source, while the occluded areas occur when the ground surface is not visible from the sensor.

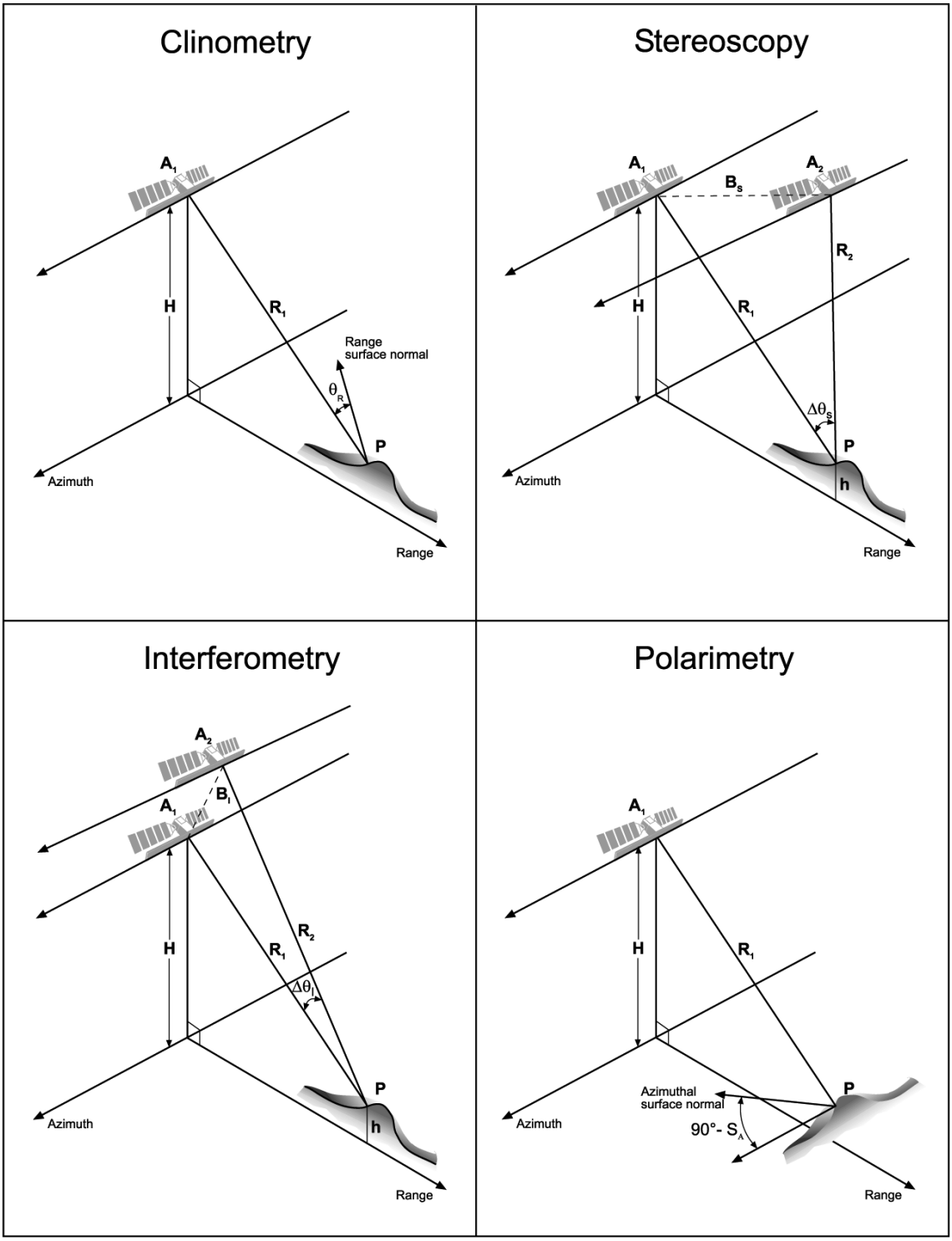

Fig. 2. Comparison of the geometry for the four elevation extraction methods: clinometry, stereoscopy, interferometry and polarimetry. A_i and H are the satellite position and altitude respectively, R the slant-range component and h the elevation of a ground point P. For clinometry, θ_R is the incidence angle in the plane defined by the range direction and the surface normal. For stereoscopy, $\Delta\theta_S$ is the intersection angle, i.e. the difference between the two incidence angles and B_S (few hundred kilometres) the baseline. For interferometry, $\Delta\theta_I$ is the difference between the two incidence angles and B_I (few hundred metres) the baseline ($\Delta\theta_I << \Delta\theta_S$; $B_I << B_S$). For polarimetry, S_A is the terrain slope in the plane defined by the azimuth and vertical directions.

Since the illumination source is the sensor with monostatic (i.e. transmit and receive antennas are together) SAR images, the effects of these two phenomena are mixed, and shadow and occluded areas are then the same. Since the shadow areas are completely without information, the boundaries of a cast shadow are then easier to determine than with visible and infrared (VIR) images. Depending on the SAR look-angles, only the steepest slopes can produce shadow/occluded areas (e.g., slopes larger than 67° and 51° for ERS-SAR and RADARSAT-F5, respectively). The shadow and layover lengths can then be consistently measured only from vertical structures, such as buildings, towers, trees etc. Consequently, the applicability of the method is reduced to very specific rugged terrain with strong cliffs. Relative heights can be derived from the cast shadow using simple trigonometric models and knowledge of the SAR geometry (La Prade and Leonardo, 1969). Since the shadow is shortened by the amount of layover due to vertical structures, the layover lengths have to be added to the shadow lengths in the computation.

Using high-resolution simulated radar images, La Prade and Leonardo (1969) determined the elevation of few man-made vertical structures (buildings and bridge towers with 100 - 200 m elevation, e.g. Empire State building and Golden Gate bridge) and hill peaks (50-150 m elevation) with an average error of 1.5% and 2.4% of the elevation, respectively. Even though the elevation modeling is coarse, this corresponds to elevation accuracy of a few meters.

2.2. Shading

Shading is the variation of brightness exhibited in images. It arises primarily because some parts of a surface are oriented so as to reflect more of the incident illumination towards the sensor (Horn, 1975). Since shading provides cues for the whole surface and not just along

special contours, the surface slope and height can be estimated, given that the surface reflectivity function and the position of the illumination source are known (see Fig. 2 top left).

The application of the clinometry concept to SAR data is less evident due to the sensitivity of shading to reflective properties of the Earth's surface. Radarclinometry, as an adaptation of photoclinometry developed by Horn (1975), has been further developed by Wildey (1984) regarding the mathematical equations, and then again by Wildey (1986) regarding its operational feasibility in anticipation of the Magellan mission to map Venus. Radarclinometry capabilities and limitations are well known, even if the research studies have been limited (Frankot and Chellapa, 1988; Thomas et al., 1989, 1991; Guindon, 1990).

At first, the principle appears simple, essentially the inversion of a mathematical expression of the radar backscatter in terms of the albedo and the local incidence angle. The local slope is then computed from the pixel reflectivity value and transformed into relative elevation by integration pixel by pixel. In other words, shape-from-shading makes use of the sensitivity of the micro-topography, but it can not provide absolute location. Some reference elevation information is needed to derive the absolute elevation. Intrinsic radiometric and geometric ambiguities then limit the accuracy of this technique, when applied to general terrain surfaces; the accuracy of derived slopes and elevation is generally of the order of few degrees and better than 100 m respectively, depending on the image resolution and terrain relief.

Firstly, the SAR backscatter of the surface changes, if the surface properties vary from place to place and assuming uniform reflecting properties (constant albedo), will recover a shape (incidence angle) that is different from the actual one. However, even with surfaces of varying reflectivity, often a Lambertian model for homogeneous surfaces is used for simplification.

This approximation was first used with SAR by Wildey (1986), and is now used in most research studies.

More sophisticated models (Ulaby and Dobson, 1988), which take into account the SAR and surface interaction (surface geometry, vegetation, soil properties, geographic conditions, etc.) have been developed. They should now permit a more realistic backscattering model of the intensity (Paquerault and Maître, 1997, 1998) than the traditional Lambertian model used for homogeneous surfaces. No attempt to extensively use these new models has been made, due to a relative decline of the interest of the scientific community in clinometry during the last ten years. Other radiometric problems, which are not completely controlled and fully resolved, are specific to SAR sensors (Guindon, 1990; Polidori, 1997), namely speckle and miscalibration.

Secondly, the geometric ambiguity is related to the definition of the incidence angle. Even if it is accurately determined, it does not define uniquely the orientation of the surface but a set of possible orientations. Their normal directions describe a cone with the axis being the illumination direction. Since there are two degrees of freedom for the surface orientation, two angles to specify the direction of a unit vector perpendicular to the surface are needed (Horn, 1975). At each pixel, one brightness measurement gives only one equation for two unknowns. Additional constraints or assumptions have to be made to resolve this conic ambiguity. One assumption implemented by Widey (1986) is the hypothesis of local cylindricity. It enforces a local continuity between adjacent pixels to define a local cylinder. Since there is no iteration in the solution process, the local-cylindricity method is sensitive to integration approximations due to miscalibration and image noise. It then tends to accumulate these effects along the full DEM reconstruction leading to “pseudo systematic” errors (Leberl, 1990). Guindon (1990)

quantified some of these aspects with a SEASAT-SAR image over a high relief terrain (1200 m elevation range with 10°-15° mean slopes); it was shown that the speckle caused large random errors in the order of hundreds of metres and miscalibration, a systematic bias in the order of tens of metres.

Other assumptions or constraints to resolve the conic ambiguity implemented by Frankot and Chellapa (1988) are the notions of integrability and regularisation. The first one states that heights can be integrated along any path, since these values are independent of the integration path. This constraint acts as a smoothing process and can reduce the slope errors by a ratio of 4 to 5. The second constraint limits the amount of allowable oscillation in the computed terrain surface, but does not significantly improve the results, perhaps indicating that most of the smoothing is coming from the integrability constraint. Furthermore, they used an iterative approach starting from a coarse existing DEM. Differences between the grey values of the real image and the SAR synthetic image, predicted from the latest estimated DEM, are used to improve the terrain slopes and heights and to converge to the final DEM. As many as 300 iterations can increase the accuracy by a factor of 5 (Leberl, 1990). This approach mainly adds details of the micro-topography to the DEM (Thomas et al., 1991). In conjunction with the integrability and regularisation constraints, this approach tends to spread out the speckle noise errors instead of propagating them only along the range profiles, leading to slope errors of 1° to 2° (only tested with simulated images).

Thomas et al. (1989) expanded this iterative approach to multiple images. Stereoscopy is first used to derive a DEM as a starting point of the shape-from-shading process. Some spot heights derived from stereoscopy or other sources can also be added as supplementary constraints of the estimated heights. Use of multi-image algorithms enables better stability and

robustness with noisy images during the iteration procedure, as well as 5 to 10 times faster convergence. Using two X-band SAR images (6 m resolution, 7 looks) acquired by the STAR-2 system of Intera Technologies Ltd., Canada over a medium relief terrain (500 m elevation range), Thomas et al. (1991) refined the radargrammetric DEM with this iterative two-image approach. As expected, the final DEM was not significantly more accurate than the radargrammetric DEM (22 m versus 25 m), but the refinement of the details in the micro-topography was evident. However, all these constraints and refined processing algorithms do not fully resolve the two basic ambiguities.

For the conic ambiguity, Guindon (1990) quantitatively demonstrated that the SAR image grey level is not an effective indicator of local incidence angle, and hence is not an accurate measure of the overall local terrain surface normal direction. It is only a strong indicator of the range component of the terrain slope. It can therefore be used only to derive elevation profiles for individual range image lines. Consequently, using a single SEASAT-SAR image over a high relief area, he only evaluated the elevation accuracy along range profiles, and obtained a slope and elevation accuracy of about 2° to 3° and 50 m to 80 m, respectively.

Since no significant detectable information is available about azimuthal slope, an additional source of "azimuthal control" data is required to tie the adjacent range line elevation profiles to a common and absolute origin. Paquerault and Maître (1997) thus developed a two-step strategy to compute these two components of the incidence angle. Firstly, they computed the range component from the backscatter pixel values, and integrated it along a range line. They then applied a contextual Markovian strategy to successively modify, in a random order, the slope orientation of each pixel in the image. This second step provided a way (i) to take into account the azimuth component of the incidence angle, (ii) to link together the adjacent range

line elevation profiles, and (iii) to reduce the noise error propagation. The method seems to be more effective than the research studies previously described, since the extracted DEMs using a single-image technique have a consistent accuracy of about 30 m for various satellite data (ERS, JERS, RADARSAT) and low-to-moderate relief terrain (200 m elevation range, 10° slopes). It is worth mentioning than these results obtained with 30 m resolution satellite images with the single-image approach, are comparable to those obtained with high-resolution simulated or airborne images with the multi-image approach. Furthermore, they noticed that the DEM accuracy is correlated not only with the elevations, but also the SAR look-angles; from 20 m to 200 m elevation the accuracy varies regularly from 13 m to 33 m, and from 25° to 45° look-angles it varies from 25 m to 32 m. Table 1 summarises the general results of elevation extraction or DEM generation with the shape-from-shading method.

Table 1
General results of shape-from-shading DEM accuracy. Low-resolution SAR (around 30 m) is for satellite images (Guindon, 1990 with SEASAT; Paquerault and Maître, 1997 with ERS, JERS, RADARSAT-Standard) and high-resolution SAR (less than 10 m) for simulated or airborne images (Thomas et al., 1989, 1991).

Method	Relief	Accuracy (m)	
		Low-Resolution	High-Resolution
Single Image	Medium	30	
	High	50 – 80	120
Multiple Images	Medium		22
	High		80

Despite the developments and the interesting results in the mid 1990s, SAR shape-from-shading remains a marginal technique, applied mainly in difficult situations such as tropical land-cover or extraterrestrial sites without ground truth. It is mainly due to the fact that the

radiometric ambiguity between the terrain albedo, the radar backscattering cross-section and the incidence angle is rarely solved, except on a homogeneous terrain surface with a Lambertian model. However, Earth parts that are not or poorly mapped approximate to a large extent a homogeneous Lambertian surface.

3. Stereoscopy

Disparity and convergence are the two cues when viewing stereo imagery. Disparity predominates when viewing radar images, but the shade and shadow cues also have a strong and cumulative effect. For example, with a quasi-flat terrain, the shade and shadow cues overcome the disparity effect when viewing pseudoscopically a radar stereo pair (Toutin and Amaral, 2000). Due to the specific geometric and radiometric aspects of SAR images, it may take our brain time to assimilate this unnatural stereo viewing, mainly when both geometric and radiometric disparities are large (Toutin, 1996). However, since depth perception is an active process (brain and eye) and relies on an intimate relationship with object recognition, after training, radar images can be viewed in stereo as easily as VIR satellite images. This disparity principle is used in radargrammetry to compute the terrain elevation from the measured parallaxes between the two images (see Fig.2 top right).

3.1. Application to SAR sensors

In the 1960s, stereoscopic methods were first applied to radar images to derive ground elevation leading to the development of radargrammetry (La Prade, 1963). He showed that some specific SAR stereo configurations would produce the same elevation parallaxes as produced by aerial images. Consequently, elevation could be measured with traditional stereo plotters. Furthermore, Carlson (1973) developed a technique to generate radar stereo images acquired form one flight path with fore and aft squinted looks, which were easier to view and

measure than the traditional technique with two flight paths. However, the lack of radar stereo pairs led mainly to theoretical studies (Rosenfield, 1968; Gracie et al., 1970; Leberl, 1979) or simulated data processing experiments (Kaupp et al., 1983; Domik, 1984).

During the 1980s, improvements of SAR systems, with parallel investigations into their theory, have allowed the demonstration of stereo radar with same-side or opposite-side viewing. These theoretical studies (Leberl, 1979) and practical experiments (Fullerton et al., 1986; Toutin, 1996) confirm that the opposite-side stereo configuration is superior to the same-side stereo. The difficulty in using this geometrically superior configuration comes from the illumination differences that are too pronounced, and thus, make stereo viewing and finding of corresponding points and features more difficult. Fig. 3 illustrates the intersection geometry with the radar elevation parallax for different stereo configurations (same versus opposite side; steep versus shallow look-angles).

To obtain good geometry for stereo plotting, the intersection angle (Fig. 3) should be large in order to increase the stereo exaggeration factor, or equivalently the observed parallax, which is used to determine the terrain elevation. Conversely, to have good stereo viewing, the interpreters (or the image matching software) prefer images as nearly identical as possible, implying a small intersection angle. Consequently, large geometric and radiometric disparities together hinder stereo viewing and precise stereo plotting. Thus, a compromise has to be reached between a better stereo viewing (small radiometric differences) and more accurate elevation determination (large parallax).

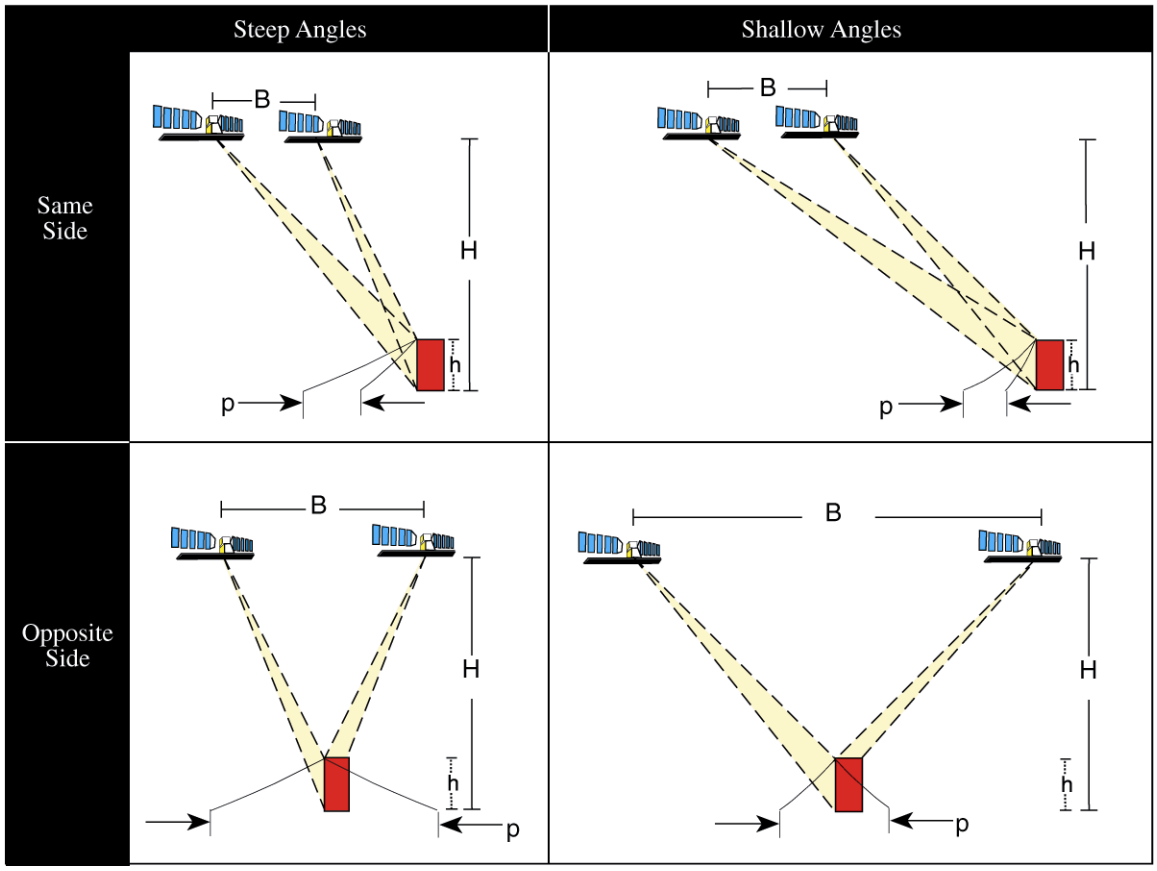

Fig. 3. The intersection geometry with the radar parallax (p) due to the terrain elevation (h) for different stereo SAR configurations (same-side versus opposite-side; steep versus shallow look-angles).

The common compromise for any type of relief is to use a same-side stereo pair, thus fulfilling both conditions above. Unfortunately, this does not maximise the full potential of stereo radar for terrain relief extraction. Different compromises can then be realised to reduce either geometric or radiometric disparities. To reduce the radiometric differences of an opposite-side stereo pair, the radiometry of one image can be inverted (Yoritomo, 1972; Fullerton et al., 1986). Fullerton et al. (1986) added a local brightness change to exclude some image features from the radiometric inversion. Another potential compromise is to use opposite-side stereo pairs over rolling topography (Toutin, 1996). The rolling topography reduces the parallax difference and also the radiometric disparities (no layover and shadow, little foreshortening) making possible simultaneously good stereo-viewing and accurate stereo

plotting. A last approach to minimise the geometric disparities is to pre-process the images using a large grid spacing or low accuracy DEM, as it has been applied with success to iterative hierarchical SAR image matching (Simard et al., 1986).

However, with spaceborne platforms, parallel flights (from opposite or same side) are very rare. Even sun-synchronous satellite orbits are parallel only near the Equator. Elsewhere, crossing orbits or convergent stereo configuration must be considered. If rigorous intersection geometry is applied, no differences exist between computations for parallel orbits and those for crossing orbits. That has been confirmed with the SIR-A/B shuttle missions of 1981 and 1984 (Kobrick et al., 1986; Leberl et al., 1986a; Simard et al., 1986). The two first studies processed radar images at an analytical stereo plotter, the Kern DSR-1, adapted to process stereo SAR images. The last study used a fully digital method with iterative hierarchical matching. The results achieved for the DEM were on the order of 60 m to 100 m mainly due to the poor SIR-A resolution, or radiometric and geometric image quality. Furthermore, the SIR-B SAR was the first system for creating and comparing different stereo pairs with ray intersection angles ranging from 5º to 23º (Leberl et al., 1986b).

Since the launch of different satellite sensors (Almaz, ERS, JERS, etc.) in the beginning of the 1990s, radargrammetry again became a hot R&D topic. The Russian Almaz-1 SAR system acquired images with different angles to obtain stereo images in the latitude range from 0º to 72º. Yelizavetin (1993) digitally processed two images with 38º and 59º look-angles over a mountainous area of Nevada, USA. No quantitative results were given. Stereoscopy with ERS-SAR data has been obtained using an image with its normal look-angle (23º) and a second image with the Roll-Tilt Mode (RTM) angle (35º) to generate a same-side stereo pair (Raggam et al., 1993). However, this ERS stereo configuration is very rare due to the limited

amount of SAR data acquired in RTM. Another ERS stereo configuration can also be used with two normal look-angle (23º) images from ascending and descending orbits to generate an opposite-side stereo pair (Toutin, 1995, 1996). Comparison of these research results (20 m versus 40 m) confirmed the superiority of the opposite-side stereo pair. With the JERS-SAR, stereoscopy can only be obtained with adjacent orbits generating a small overlap with a weak stereo configuration (ray intersection angle less than 4°) that cannot be used in a low-to-moderate relief terrain. Using a digital matching method, Raggam and Almer (1996) achieved DEM accuracy of 75 m over a mountainous area in the Austrian Alps.

These reported results are generally inconsistent and practical experiments do not clearly support theoretical expectations. For example, larger ray intersection angles and higher spatial resolution do not translate into higher accuracy. In various experiments, accuracy trends even reverse, especially for rough topography. Only in the extreme case of low relief, does accuracy approach the theoretical expectations. The main reason is that the error modeling accounts only for SAR geometric aspects (look and intersection angles, range error) and completely neglects the radiometric aspects (SAR backscatter) of the stereo pair and of the terrain. This error propagation modeling can thus be applied only when the radiometry has a minor role and impact with respect to the geometry, such as in a stereo-model set-up with GCPs, which are radiometrically well-defined points (Sylvander et al., 1997; Toutin, 1998). The residual error of the least square bundle adjustment of the stereo model parameters is thus correlated with the intersection angle.

Since SAR backscatter, and consequently the image radiometry, is much more sensitive to the incidence angle that the VIR reflectance, especially at low incidence angles, the possibility of using theoretical error propagation as a tool for predicting accuracy and selecting appropriate

stereo-images for DEM generation is very limited. Therefore, care must be taken in attempting to extrapolate VIR stereo concepts to SAR.

Previously to RADARSAT, Canada's first earth observation satellite launched in November 1995, it was difficult to acquire different stereo configurations to address the above points. RADARSAT with its various operating modes, imagery from a broad range of look directions, beam positions and modes at different resolutions (Parashar et al., 1993) fills this gap. Under the Applications Development and Research Opportunity (ADRO) program sponsored by the Canadian Space Agency, researchers around the world have undertaken studies on the stereoscopic capabilities by varying the geometric parameters (look and intersection angles, resolution, etc.). Most of the results were presented at the final RADARSAT ADRO Symposium "Bringing Radar Application Down to Earth" held in Montreal, Canada in 1998. There was a general consensus on the achieved DEM extraction accuracy: a little more (12 m) for the fine mode, and a little less (20 m) than the image resolution for the standard mode, independently of the method used (digital stereo plotter or image matching). Relative elevation extraction from a fine mode RADARSAT stereo pair for the measurement of canopy heights in the tropical forest of Brazil was also addressed (Toutin and Amaral, 2000).

In fact, most of the experiments showed that the principal parameter that has a significant impact on the accuracy of the DEM is the type of the relief and its slope (Toutin, 2000a). However, there were no significant correlations between the DEM accuracy and the intersection angle in the various ADRO experiment results. This confirmed the contradiction found with SIR-B (Leberl et al., 1986b). The greater the difference between two look-angles (large intersection angle), the more the quality of the stereoscopic fusion deteriorated. This

cancels out the advantage obtained from the stronger stereo geometry, and this is more pronounced with high-relief terrain. On the other hand, although a higher resolution (fine mode) produced a better quality image, it does not change the stereo acuity for a given configuration (e.g. intersection angle), and it does not improve significantly the DEM accuracy. Furthermore, although the speckle creates some confusion in stereo plotting, it does not degrade the DEM accuracy because the matching methods or the human stereo viewing "behave like a filter". Preprocessing the images with an adaptive speckle filtering does not improve the DEM accuracy with a multi-scale matching method (Dowman et al., 1997); it can slightly reduce the image contrast and smoothes the relief, especially the low one (Toutin, 1999).

Since the type of relief is an important parameter influencing the DEM accuracy, it is strongly recommended that the DEM accuracy be estimated for different relief types. Furthermore, in the choice of a stereoscopic pair for DEM generation, both the geometric and radiometric characteristics must be jointly evaluated taking into account the SAR and surface interaction (surface geometry, vegetation, soil properties, geographic conditions, etc.). The advantages of one characteristic must be weighted against the deficits of the other. Table 2 summarises the general results of DEM generation with stereoscopy.

3.2. Combined sensors

Due to the increasing amount of sensors, it is very common to have data from different sensors over the same area. The traditional stereoscopic technique can be applied also with such data. By combining the different radiometry in the brain, the stereoscopic fusion of combined data can provide a virtual 3D model of the terrain surface. Few results have been published on the use of combined stereo VIR and SAR sensors to generate DEMs.

Table 2

General results of radargrammetric-DEM accuracy

Satellite	SAR Band-Polarisation	Resolution (m)	Relief Type	Accuracy (m) Same-Side	Opposite-Side
SIR A	L-HH	25	High	100	
SIR B	L-HH	40	Medium	25	
			High	60	36
ERS 1/2	C-VV	24	Medium	20	20
			High	45	
JERS	L-VV	18	High	75	
Almaz	S-HH	15	High	30-50	
RADARSAT	C-HH	F[a] 7-9	Low	8-10	20
		S[a] 20-29	Medium	15-20	40
		W[a] 20-40	High	25-30	

[a] F, S, W …fine, standard, wide imaging modes

Moore (1969) first addressed the principle theoretically, by using simultaneously infrared line-scanner and SLAR images. The visual stereo effect was not perfect except near 45° viewing angle. Various scaling factors were also applied to different areas of the stereo pair to obtain a proper stereo effect for height determination. No quantitative measurement was realised due to the lack of an "adapted" stereo plotter.

Further evaluation has been realised with SIR-B and Landsat-TM images (Bloom et al., 1988). Approximate error evaluation showed moderate results (in the order of 100 m) for 27 extracted points (sharp ridge crests), mainly due to image resolution, different object appearance, errors in the image registration and the imprecise look angles used in the simplified elevation computation equation. Using a better parametric solution, Raggam et al.

(1994) extracted a DEM from a multi-band SPOT and airborne SAR stereo pair. Since no meaningful results can be obtained from automatic image matching, they interactively measured 500 corresponding image points without stereoscopic capability and computed the elevation off-line. Results of the comparison with a reference DEM showed a standard deviation of 60 m with a 42-m bias and minimum/maximum error of about ±250 m. More recently, Toutin (2000b) further investigated the mapping feasibility of combined sensor stereo pairs with parametric geometric solutions ported to a digital stereo-workstation adapted to process on-line VIR and SAR stereo pairs. From the raw images (no epipolar resampling), the data are interactively extracted, and then directly compared to a checked DEM. An accuracy of 20 m with no bias and minimum/maximum errors of less than ±100 m has been achieved from two different SPOT-PAN and ERS-SAR stereo pairs: one being an opposite-side stereo pair and the other a same-side stereo pair. The full on-line stereo capabilities in the GCP plotting and elevation measurements account for the good results. Comparisons of the two stereo pair results showed that the elevation parallax, which contributes to the determination of the elevation, is dominated mainly by the SAR geometry with its high sensitivity to the terrain relief. Conversely, the SPOT-PAN images mainly contribute to the easier identification of features, due to the better image quality and higher spatial resolution.

3.3. Processing, methods and errors

The different processing steps to produce DEMs using stereo-images can be described in broad terms: (i) acquiring stereo-images, (ii) collecting GCPs and stereo-model set-up, (iii) extracting elevation parallaxes and computing 3D co-ordinates.

3.3.1. Acquiring stereo-image data

The SAR images are standard products in slant- or ground-range forms. They are generated

digitally during post-processing from the raw signal SAR data (Doppler frequency, time delay). The ground-range form is more popular, since the pixel spacing on the ground is roughly the same for the different look-angle images. This facilitates stereo viewing and matching. The geometric modeling solution to compute the stereo model and 3D intersection starts generally either from the projection equations generalised for different scanning sensors (Leberl, 1972; Toutin, 1995), from the Doppler and range equations (Dowman et al., 1997; Sylvander et al., 1997), or from the equations of radargrammetry based on the radar image geometry (Leberl, 1990; Raggam et al., 1993). More details on the physical principles, mathematical formulations and differences of these three methods can be found in the given references.

3.3.2. Collecting GCPs and stereomodel set-up

Independently of the SAR geometric modeling used, some GCPs are needed to refine the stereo model parameters with a least square bundle adjustment process in order to obtain a cartographic-standard accuracy. With a geometric modeling solution such as defined in Section 3.3.1, few GCPs (1 to 4) are required. In an operational environment, their number will vary as a function of their accuracy. They should preferably be located at the border of the stereopair to avoid extrapolation in planimetry, and should cover the full terrain elevation range. Height control points and tie points can be added to strengthen the stereo geometry.

The final accuracy of the stereo geometry is mainly dependent on the GCPs ground and image co-ordinates. The first can be obtained from GPS, aerial image surveys, map digitising, etc. The image co-ordinates are measured interactively at the plotter or the computer monitor. Since some workstations do not have full stereoscopic capabilities, the image co-ordinates are then measured monoscopically. Image co-ordinate measurement errors can be large with a

SAR stereo pair (ca. 1-2 pixels) and influence the DEM accuracy. Due to the same-side geometry with small intersection angles (8º to 20º) of SAR stereo pairs, the propagation of the monoscopic measurement errors increases with shallower look-angles and smaller intersection angles (Toutin, 1998). Consequently, the DEM accuracy can decrease by 20% to 40%, depending on the stereo-pair geometry (Toutin, 1999, 2000a). Stereoscopic measurement leads to more accurate image co-ordinates and elevations.

3.3.3. Extracting elevation parallax

Two methods can be principally used to extract the elevation parallax using image matching: computer-assisted (visual) or automatic methods. These two methods can be integrated to take into account the strength of each one.

The computer-assisted visual matching is an extension of the traditional photogrammetric method to extract elevation data at a stereo plotter. It requires full stereoscopic capabilities with 3D viewing devices to generate on-line the 3D reconstruction of the stereo model, to capture and to edit in real-time 3D elevation features. More details on SAR stereo workstations and their 3D capabilities can be found in Dowman et al. (1992).

To view the images in stereo, the images are resampled into an epipolar or quasi-epipolar geometry, in which only the X-parallax related to the elevation is retained. Another solution to achieve stereo viewing using the raw images is to automatically and dynamically remove the Y-parallax at the floating mark position (Toutin, 1995). Image measurement and computation of ground co-ordinates are performed as with conventional stereo plotters. Some automated tasks (displacement of the images or cursors, prediction of the corresponding image point position, etc.) may be added.

However, computer-assisted visual matching to derive DEMs is a long and expensive process. Thus, when using digital images, automated image matching can be used. Since image matching has been an active research topic for the last twenty years, an enormous body of research work and literature exists on stereo matching.

The first generation of image matching methods is grey-level image matching (Marr and Poggio, 1977). Although satellite images are not like a random-dot stereogram (easily matchable), grey level matching has been widely studied and applied to SAR data. Grey level matching can be computed with the normalised cross-correlation coefficient (Simard et al., 1986; Sylvander et al., 1997), the sum of mean normalised absolute difference (Ramapriyan et al., 1986), a least squares solution (Dowman et al., 1997), etc. The first one is considered to be the most accurate (see Leberl et al., 1994) and is commonly used with SAR images. Furthermore, a hierarchical strategy is sometimes implemented to reduce the SAR image noise and the elevation parallaxes, which enables to derive an approximate DEM at each image pyramid level (Dowman et al., 1997; Toutin, 1999).

Marr also developed a second generation of image matching: feature-based matching (Marr and Hildreth, 1980). The same object may look considerably different in SAR images acquired at different times and with different geometric relationships between the SAR transmit and receive antenna and the terrain. But, according to Marr's theory, image edges reflect generally true object structures. However, feature-based matching has not been very popular with SAR images because edges in mountainous terrain may differ a lot from one image to the other.

Thus, hybrid approaches can be realised to achieve better and faster results by combining grey-level matching and feature-based matching with a hierarchical multi-scale algorithm, but also with computer-assisted visual matching. The feature-based approach may produce good results for well-defined features, but no elevation values in-between. These results can then be used as seed points for grey-level matching. Another hybrid approach is to generate in a first step grey-value gradient images instead of binary edge images. Then, any grey-level matching technique can be used on these preprocessed images (Paillou and Gelautz, 1999). The linear gradient operator used by them was designed to be optimal to remove noise (such as SAR speckle) and enhance edges. Their first preliminary results with SAR stereo images show 10-15% improvement in the DEM reconstruction, not always significant or consistent, but at least with less blunders due to the noise removal.

Although the computer-assisted visual matching is a long process, it has been proven to be more accurate with SAR data (Leberl et al., 1994; Toutin, 1999) or with combined sensors (Raggam et al., 1994; Toutin, 2000b). Thus, it could be used to add new points in areas with sparse measurements, eliminate blunders, and correct mismatched areas or areas with errors larger than one pixel (about 40 to 50%, Leberl et al., 1994). It could also be used to generate seed points for the automatic matching.

4. Interferometry

Radar interferometry is an alternative to the conventional stereoscopic method for extracting relative or absolute elevation information. It uses the coherent property of modern SAR and enjoys the advantages of radar systems and of digital image processing: all-weather, night and day operation, and automated or semi-automated processing. Imaging interferometric SAR (InSAR) combines complex images recorded either by two antennas at different locations, or

with the same antenna at two different times (see Fig. 2 bottom left). If the same antenna is used at two different times then the location difference must be small, normally less than a kilometre for satellite repeat-pass interferometry. The phase difference information between the SAR images is used to measure precisely changes in the range, on the sub-wavelength scale, for corresponding points in an image pair. Analysis of the differential phase, and therefore change in distance, between the corresponding pixel centres and the observing antenna can lead to information on terrain elevation or, with observations with the same antenna at different times, terrain displacement.

Apart from airborne demonstration at the Jet Propulsion Laboratory (JPL) in Pasadena, USA spaceborne SEASAT data was used by Li and Goldstein (1990) to show the feasibility of combining data from pairs of passes for the derivation of height information. The technique was extended to SIR-B data acquired from two separate Shuttle passes acquired over several days (Gabriel and Goldstein, 1988). The exciting early observation of in-scene relative movement was also made at JPL by Gabriel et al. (1989), although the first quantitative demonstration that millimetre scale movement is measurable with radar interferometry was shown by Gray and Farris-Manning (1993) at the Canada Centre for Remote Sensing (CCRS) using airborne repeat-pass interferometry. After the launch of ERS-1 in 1991, numerous multi-pass satellite interferometric studies have been realised (Massonnet and Rabaute, 1993), subsequently with Almaz-1 (Yelizavetin and Ksenofontov, 1996) and with RADARSAT (Geudtner et al., 1997). Although the early emphasis in the research with satellite InSAR data was on the estimation of terrain topography, there has been increasing work on use of InSAR techniques for measuring terrain movement and change: with ERS-1/2 (and tandem mode data), SIR-C, RADARSAT, and with data from the Japanese satellite JERS-1. This work has been recently reviewed by Massonet and Feigl (1998).

With existing satellite SAR sensors, only the repeat-pass system (one satellite antenna and two passes of the satellite) can generate interferometric data through the combination of complex images since there is presently no satellite system with two antennas. Such a dual-antenna system, the Shuttle Radar Topographic Mission (SRTM) has been launched in early 2000. Although this system provides 100-m grid spacing DEMs of a large fraction of the Earth's surface, in the following we concentrate on the methodology and accuracy of DEM generation using repeat-pass InSAR with existing satellite sensors.

Before outlining the processing stages in satellite repeat-pass InSAR, it is important to understand the conditions necessary for interferometry, and to be able to select pairs of passes which may have the necessary properties for the creation of useful geophysical information. The imaging geometry of the first pass must be repeated almost exactly in the second pass. The concept of the critical baseline was introduced (Gabriel and Goldstein, 1988; Massonnet and Rabaute, 1993) to describe the maximum separation of the satellite orbits in the direction orthogonal to both the along-track direction and the radar range direction. This separation is usually referred to as the perpendicular baseline. If this critical value is exceeded, one would not expect clear phase fringes or adequate "phase coherence". The sensitivity to terrain topography increases with the perpendicular baseline so that there is an optimum baseline for DEM generation. This is in contrast to the use of InSAR for terrain movement in which a very small baseline is clearly optimum to avoid problems with topography. In practice, the optimum baseline is terrain dependent as moderate to large slopes can generate an aliased phase rate or a phase that can be difficult to process in subsequent stages such as phase unwrapping. Normally, a baseline between one third and one half of the critical baseline (i.e. around 300 m to 500 m for ERS data) is good for DEM generation, if terrain slope is

moderate. In mountainous regions a smaller baseline would be more appropriate. RADARSAT has three options for the slant-range resolution, which are changed for the various modes (Parashar et al., 1993). In particular, use of the fine-resolution mode relaxes the criterion for the critical baseline and it is possible to use baselines of 1 km or even larger. This increases the sensitivity to topography and can lead to a more accurate DEM product than with the lower resolution modes of RADARSAT or ERS (Vachon et al., 1995).

Also, the difference in orientation of the imaging planes (the planes containing the line-of-sight and vertical directions) must be less than the azimuth beam width. This is most easily confirmed by checking the "Doppler parameters" used in the SAR data processing; there must be an overlap in the azimuth spectra. Orbit maintenance and attitude control of most satellites is such that this requirement is rarely a problem. It is possible to reduce the noise in the differential phase image through band-pass filtering in both range and azimuth directions (Prati and Rocca, 1993).

The complex SAR images are registered and the phase difference is computed for each pixel. Registration can be accomplished in a number of ways, either based on cross-correlation of the image radiometry (speckle correlation), or by optimising phase patterns or coherence for areas extracted from the two images. The product of one complex image times the complex conjugate of the second image is the primary product in InSAR work and is often referred to as an interferogram, although some authors prefer to use this term for a normalised product or even a phase difference image. If the backscatter has not changed significantly over the time between acquisitions, the phase of the interferogram is not random but contains information on the differential range from the object pixel to the SAR antenna in the two passes. There is a stereoscopic component in the differential range that should be removed from knowledge of

the orbit data. This is sometimes referred to as the "flat Earth correction" stage. Further, it is also advantageous to use even a coarse-resolution DEM to remove some of the phase variations due to topography. After the flat Earth and first order topographic corrections have been made to the phase of the interferogram one can now carry out an averaging in the complex domain and be more confident that the process will not corrupt the phase. The averaged interferogram can be used to provide a multi-look image, as well as an image of a secondary product, i.e. the coherence. The maximum value for the coherence is 1, corresponding to all pixels in the window having the same phase. Unfortunately, the coherence depends on the size of the window used in its calculation (Touzi et al., 1999) and the reader is cautioned in comparing quantitative values from different experiments, unless the procedure is well described.

The phase of the averaged interferogram is known only between $-\pi$ and $+\pi$. It is necessary to "unwrap" the phase difference to estimate how the differential range changes across the image. Often there are areas of lower coherence and higher phase noise, which lead to problems with phase unwrapping. One approach in avoiding the problem of error propagation when the phase is unwrapped incorrectly is to identify phase "residues". If one integrates the phase over a closed path, the sum of the phase values should be zero. If the value is closer to a multiple of 2π this indicates a phase residue, and unwrapping across a line connecting adjacent residues should be avoided (Goldstein et al., 1988). Phase unwrapping remains an area of active research and many approaches have been suggested (Ghiglia and Pritt, 1998). Notwithstanding the effort that has been invested in this part of InSAR processing, it can be rarely executed in a totally automated fashion. Quality control of the unwrapped phase should be done to look for phase jumps and inconsistencies in the output. If necessary, areas of low coherence and high phase noise can be blocked out and phase unwrapping completed around

them.

The terrain elevations can be derived from the unwrapped phase, the baseline information, beam-pointing information (from Doppler parameters), and an Earth model (usually an ellipsoid). If an initial DEM was used to reduce the fringe rate and improve the range filtering for slopes, then of course the solution would be the additional topographic variation. This process is often based on the SAR geocoding work of Curlander (1982). In principle, the process can be completed without recourse to ground control points but in practice some ground control is important to reduce the need for precise orbit information. Control points are normally used to refine the baseline model used in the phase to height algorithm. The baseline is not constant for a scene, and usually the refinement can be modelled as a linear change in the vertical and horizontal direction. In one careful, systematic study of InSAR derived topography (Small et al., 1995) the accuracies for height determination were 2.7 m RMS for relatively small areas, a 12 km by 13 km area close to Bonn, Germany, and only small biases were observed over a 40 km by 50 km scene. However, the presence of different propagation conditions during data acquisition can affect the differential phase and degrade the results. Small changes of the actual baseline can be used to compensate for different large scale propagation conditions during the two acquisition dates (Tarayre and Massonnet, 1996).

Various propagation effects can corrupt the differential phase and create errors in an interferometric product. These have been largely described by various authors (Goldstein, 1995; Massonet and Feigl, 1995; Tarayre and Massonet, 1996). The usual culprit is variations in atmospheric water vapour in the troposphere, which retards the propagation and leads to an additional phase variation, which corrupts interpretation of the differential phase in terms of topography or surface motion. Ionospheric effects can also lead to InSAR errors (Tarayre and

Massonet, 1996) although these effects are more probable near the equator and in polar regions. Even tests of interferometric mapping in the high Arctic in winter have revealed modulations in a height error map (a comparison of airborne and spaceborne InSAR derived DEMs), which appeared to be related to variations in atmospheric water vapour (Mattar et al., 1999).

There are a number of approaches to both recognising these effects and in adopting a strategy to minimise the errors. Ferretti et al. (1999a) show that combining multiple interferograms can improve the quality of a DEM product as well as simplify phase unwrapping. By looking for time coincident weather data it may also be possible to exclude passes which include heavy cumulonimbus clouds or rain. Another simple strategy is to work with as large a baseline as possible. In this way the phase error associated with the propagation inhomogeneity leads to a smaller error in elevation. This strategy was used to show the strength of RADARSAT fine mode InSAR in a dry Arctic environment in comparison to some ERS tandem modes pairs with much smaller baselines (Mattar et al., 1999).

Although propagation effects can limit the accuracy with which a DEM can be generated with satellite SAR interferometry, the limitation imposed by temporal coherence is more fundamental. Coherence will vary with frequency and with time but experience with C-band data shows that the rate of coherence loss varies widely dependent on the terrain (Zebker and Villasenor, 1992). Even the C-band ERS tandem mode data with one-day separation has not yielded good results for tropical rain forest, but other dry areas have shown coherence over very long periods, on the order of one year (Massonet and Feigl, 1998). As RADARSAT has a repeat cycle of 24 days, this represents a limitation for the exploitation of interferometry, although useful results have been obtained for dry terrain. Ferretti et al. (1999b) have shown

that using phase results from specific "permanent scatterers" (man-made structures, large rocks, etc.) that are stable can extend the time period over which useful measurements can be made, even if most of the scene has lost coherence usually due to vegetation and moisture change.

Current developments also include the use of satellite radar interferometry to study dynamic phenomena and their relative elevation displacement (differential interferometry). Combining a SAR interferogram generated from two ERS-1 SAR data acquired before and after an earthquake with a DEM, the topographic component is removed from the interferogram, and the displacement field map of an earthquake can be drawn (Massonnet et al., 1993). Topographic and displacement components can be also separated by combining three radar images to generate two interferograms (Zebker et al., 1994). The estimation of the displacement field using radar data alone, without any terrain information is then possible. Similarly, using repeat-track interferometry with a very small cross-track baseline, which generates interferograms with little sensitivity to topography (small topographic component), Goldstein et al. (1993) measured and estimated ice sheet motion. This technique is currently applied with RADARSAT data from the Antarctica mapping mission to measure ice motions (Gray et al., 1998) and to analyse glacier flow dynamics (Forster et al., 1998).

So far, the atmospheric component and the image coherence are the main limitations of the interferometric method for operational DEM generation. The coherence image has also been used as SAR interferometric signature for land-use classification with ERS-1 SAR repeat-pass data (Wegmüller and Werner, 1995). The interferometric coherence over forested areas was found to be significantly lower than over open canopies, small vegetation, bare soils and urban areas. The results strongly support deforestation studies, forest mapping and monitoring

since it was possible not only to distinguish coniferous, deciduous and mixed forest stands, but also regrowth and clear-cut areas.

Although these results indicated that the scene coherence over forested areas was low, the interferometric technique can still be used to estimate the topography and tree heights in specific conditions, such as a boreal forest in wintertime where the coherence varied from 0.2 to 0.5 (Hagberg et al., 1995). The interferometric phase information used to estimate the tree height relative to an open field and compared with in-situ measurements demonstrated that the scattering centre at C-band is close to the top of the trees if the forest is dense. The good coherence obtained is also a result of the stiffness of the "frozen" branches on the top of the boreal forest during the wintertime. They also noticed increased sensitivity of the degree of coherence to other environmental parameters (temperature, precipitation, snowfall and soil moisture change). Table 3 summarises the general results of DEM extraction with interferometry. The accuracy figures given there are an indication of the expected error range due to all sources: noise, baseline, propagation effects, etc. As with stereo SAR, results from low relief terrain (lowest values) will be better than those from areas with significant relief (highest values) although no quantitatively evaluation has been done. Quantitative tests of the accuracy of RADARSAT standard mode InSAR are somewhat limited, but when good coherence and suitable baselines are obtained, then accuracy should be comparable to that obtained from ERS.

Table 3

General results of interferometric-DEM accuracy. As with stereo SAR, results from low relief terrain (lowest values) will be better than those from areas with significant relief (highest values), although no quantitative evaluation has been done on this topic. Quantitative tests of the accuracy of RADARSAT standard mode InSAR are somewhat limited, but when good coherence and suitable baselines are achieved, then accuracy should be comparable to that obtained from ERS

Satellite	Resolution (m)	Accuracy (m)	Notes
ERS 1/2	24	3-20	For most areas, except tropical forest or regions with significant vegetation or moisture variability. The ERS 1/2 tandem data archive is extensive.
JERS	18	10-20	L-band shows better coherence (for more terrain types and for longer time periods) than C-band.
RADARSAT (standard mode)	20-29	10-20	Dry terrain is preferred due to the 24-day orbit repeat cycle and potential loss of coherence.
RADARSAT (fine mode)	7-9	3-10	Dry terrain preferred. Larger baselines are possible, increasing accuracy and reducing sensitivity to propagation effects.

5. Polarimetry

SAR polarimetry has been used with success for thematic classification studies involving natural scenes and man-made targets. A recently developed application of SAR polarimetry involves both a direct measure of terrain azimuthal slopes (see Fig. 2 bottom right) and a derived estimate of the terrain elevations (Schuler et al., 1996). The method is mainly based on empirical comparisons, supported by preliminary theoretical analysis, between the terrain local slope and the co-polarised signature maximum shift. This has been validated over different geographical areas and different types of natural targets using different DEMs as reference. Although it was only tested with airborne P- and L-band SAR platforms, it is worth to mention, since future satellite missions (RADARSAT-2) will generate full polarimetric SAR data.

Polarimetric SAR measures the amplitude and phase terms of the complex scattering matrix. Based on a theoretical scattering model for tilted, slightly-rough dielectric surfaces (Valenzuela, 1968), azimuthal surface slope angles and signature-peak orientation displacements produced by such slopes are proportional over a range of azimuthal slopes. Schuler et al. (1993) first demonstrated that the resolved azimuthal wave-tilts produced significant and predictable displacements in the location of the maxima of the co-polarised signature of ocean backscatter. They then hypothesised that an azimuthal angle of an open-field terrain caused a proportional shift of the co-polarised polarimetric signature maximum from its flat position by an angle almost equal to the terrain slope. Azimuthal direction slopes can then be computed from the polarimetric SAR data without any prior knowledge of the terrain. By integrating the slope profiles in the azimuthal direction relative terrain elevation can be derived. To obtain absolute elevation, one elevation point must be known along each slope profile.

Since forest scattering is more complex than open-field terrain scattering, radiative transfer models or discrete scatter formulations (Durden et al., 1989) of forest backscatter from a sloping terrain have to be used to modify the open-terrain algorithm. Schuler et al. (1996, 1998) carried out experiments with airborne NASA/JPL AIRSAR polarimetric P-band SAR data (resolution 6.6 m in range by 12.1 m in azimuth, 4 looks) over forested areas and medium relief terrain (slopes of generally 0° to 5° but up to 30°). Digital surface models (DSMs), which take into account the canopy height, are used as reference data, and also to provide the starting elevation point for each azimuth profile. Accuracies of 3° to 5° and 20 m to 30 m with high correlation coefficients (0.8-0.9) were obtained for the slopes and elevations, respectively. They are correlated with the terrain relief: for the lowest (0° to 5° slopes) and

highest (15° to 25° slopes) relief, accuracies of 8 m to 20 m and 30 m to 40 m were obtained, respectively. The canopy height may not account for part of these errors, since the elevation of "starting" points for each profile to integrate the slopes into elevations have been extracted from DSMs (including the canopy height). Furthermore, attempts to use shorter wavelength radars (C- or L-band) yielded profiles with larger errors for forested terrain, mainly for the C-band (Schuler et al., 1996). The larger slope error indicates that canopy and/or branch scattering is then dominant over the terrain relief scattering.

The technique has also been applied with AIRSAR L-band SAR data over flat desert terrain with some rugged mountains (500 m elevation range with up to 50° slopes) devoid of trees (Schuler et al., 1996). To be representative of an open-field terrain, a simplified closed form approximation to the relationship between the co-polarised maximum shift and the measured co-variance matrix elements is first established. Co-variance matrices generated from experimental or modeling data can then be used as input parameters to derive the link with the terrain azimuthal slope. Two azimuthal profiles were compared to a very accurate DEM, which is also used to integrate the elevation along profile. The achieved accuracies were 2.5° to 3.5° and 6 m to 24 m for the slopes and elevation, respectively; the lowest values for the desert terrain and the highest ones for the mountain range.

Since a DEM is not normally available in an operational environment when applying this method, sets of elevation profiles spaced throughout the range direction have to be available to obtain two-dimensional topographic elevations maps. Two orthogonal-pass SAR data is thus a solution to generate an elevation surface with only one elevation point (Schuler et al., 1998). The elevation surface may be generated as an iterative solution of a Poison-type differential equation. Using orthogonal two-pass AIRSAR L-band SAR data acquired over an

open desert terrain with some mountain range (400 m elevation range) having little ground cover, DEM results showed an accuracy of 29 m. However, 6 m accuracy was achieved in the flat desert terrain. Part of these errors was caused by registration errors and by significant changes in data quality between the two passes. Since these last results are about the same as those obtained from one pass, the two-pass technique is mainly useful to reduce the number of elevation tie-points to one. Furthermore, orthogonal passes cannot be obtained with sun-synchronous satellites (except close to the poles). Shape-from-shading techniques, which generate slopes in the across-track direction, could then be another solution. Table 4 summarises the general results of elevation extraction or DEM generation with polarimetry, only from airborne SAR data.

Table 4

Results of polarimetric-DEM accuracy with NASA/JPL's AIRSAR data. There was no test realised with two passes over forested area. There was no accuracy evaluation for the whole desert area with one pass technique (Schuler et al., 1996). There was also no explanation why with the two-pass technique over the desert area, the accuracy for the whole area (29 m) is worse than the accuracy of the other relief classes (6 m and 18 m) (Schuler et al., 1998)

Study Site	SAR Band	Resolution (m)	Relief	Accuracy (m)	
				One Pass	Two Passes
Forested area	P	6.6 x 12.1	Low-Medium	10-20	
			High	30-40	
			Whole area	20-30	
Desert area	L (1 pass) P (2 passes)	6.6 x 12.1	Low-Medium	6	6
			High	24	18
			Whole area		29

However, to apply this technique (one pass or two quasi-orthogonal passes) with satellite SAR data (mainly C- and X-bands) future work should be directed towards an analysis based on a volume scattering to take into account the more complicated situation of the SAR backscattering in forested or agricultural areas. With such scattering models, quantitative slope and elevation values could be derived from the relationship between radiation frequency, incidence angle and type of scatterer. However, the main drawbacks of this emergent technique are the volume scattering models but also the limited availability of polarimetric data to evaluate the robustness of the technique with different topographic and land-cover situations.

6. Concluding remarks

Elevation modeling from satellite data has been an active R&D topic in the theoretical development for the last thirty years and in the practical experiments for the last twenty years with the appearance of the first civilian remote sensing satellite. SAR data in different formats (analogue but mainly digital) can be processed by different methods (clinometry, stereoscopy, interferometry, polarimetry) taking advantage of the different sensor and image characteristics (geometric, radiometric, phase) using different types of technology (analogue, analytical, digital) and processing (interactive, automatic).

Most of the techniques have been proposed and addressed in the early years. However, the limited availability of data and associated technologies has restricted their evolution in comparison to traditional photogrammetry. Their respective evolution is a function of the research effort in terms of physical parameter modeling and data processing.

The shadowing method, providing localised cues along special contours is principally used to derive relative elevation of a specific target. Despite good results, the method remains limited to specific applications. Conversely to shadowing, shading provides cues all over the studied surface, but can be applied successfully only with homogeneous surfaces. Combined with the empirical approach to resolve the different ambiguities, this method also remains marginal, whatever its potential accuracy. Both methods have generated limited interest in the scientific community. On the other hand, stereoscopy is the most preferred and used method in the mapping, photogrammetry and remote sensing communities, most likely due to the heritage of the well-developed stereo photogrammetry. Advances in computer vision to model human vision has led to the advent of new automatic image processing approaches applied to satellite stereoscopy. It has thus allowed the mapping process to become more automated, but not completely due to occasional matching failures. Inversely, radar polarimetry stays mainly at the level of scientific interest on the physical parametric modeling without much effort on data or image processing development.

Their evolution in relation to the scientists' interest is also a function of the predominant "fashion". SAR stereoscopy was popular around the 1980's with the development of radargrammetry equations and the first interesting and promising results with SIR-B. However, the SAR image processing and related technologies to extract elevation data (such as image matching) were not mature enough and led to a temporary decline. In the same way, most of the R&D in shape-from-shading methods was performed in the 1980s starting with the Venus radar mapper. Similar developments applied to SPOT data took place at that time, with enormous research around the world both for physical parametric modeling and image processing, taking also advantage of the R&D in digital photogrammetry.

When ERS-1 was launched, scientists became enthusiastic over interferometric techniques because of the apparent high accuracy for DEM extraction. In the first years, most of the research efforts have focused on image processing, particularly phase unwrapping and few on the problems of atmospheric propagation and use of height control.

With the launch of RADARSAT in 1995, radargrammetry experienced a revival of the scientists' interest, taking advantage of the R&D on image matching realised for SPOT at the end of the 1980s and the new computer technologies. R&D at the dawn of the next millennium will be focused on the use of the high-resolution SAR satellites and the development of their associated technologies, such as ENVISAT, RADARSAT- 2 and the SRTM.

Since any sensor, system or method has its own advantages and disadvantages, solutions to be developed in the future for operational DEM generation should use the complementarity between the different sensors, methods and processing. It has already been used in stereoscopy combining VIR and SAR data, where the radiometric content of the VIR image is combined with the SAR high sensitivity to the terrain relief and its "all-weather" capability to obtain the second image of the stereo pair.

Based on the same philosophy, other complementary sensor data can be used:

1. Two SAR stereoscopic pairs from ascending and descending orbits to partially complement shadow and layover areas of each stereo pair;
2. Two interferometric pairs, one with a small baseline (to help the phase unwrapping), and the other with a larger baseline (to increase the accuracy); and
3. Two polarimetric images from ascending and descending orbits to resolve the across-track

ambiguity and reduce the required number of known elevation points.

The complementarity of methods has already been tried with SAR where stereoscopy is used to generate seed points needed for the clinometry or to generate an approximate DEM to help the phase unwrapping in interferometry. The loss of coherence with interferometry in forested areas can be complemented with clinometry, which is well suited to the homogeneity of the forest cover. Clinometry and polarimetry could be combined since the first one gives elevation information in the range direction and the second one in the azimuthal direction. Only one polarimetric SAR image could thus be necessary. A shadow-based method to extract building or tree heights could also be used to transform a stereoscopic or interferometric DSM into a DEM, or the reverse.

The complementarity can also be applied at the processing level: (i) using visual matching to measure seed points for the automatic matching or to postprocess and edit raw DEMs (occlusion, shadow or mismatched areas), or (ii) using stereo measurements of geomorphologic features (thalweg and crest lines, lake surfaces, etc.) to increase the mapping consistency of the DEM. Furthermore, it has been proven in most of the previous experiments that the user has to make judgements and decisions at different stages of the processing, regardless of the level of automatic processing to obtain the final DEM product: the “know-how” of the users could favourably complement the computer capability in different processing steps.

In the past, high-quality DEMs have been generated with traditional photogrammetry in such a way that they were used for many purposes. Presently, DEMs are considered the most permanent and reusable geo-related dataset over time. Although the need, requirements and

specifications of DEM products are difficult to determine due to its multiple uses by different user communities, a global DEM generation is realised with the SRTM, a US/German Space Radar Laboratory embarking on a US shuttle mission launched in February 2000. It will use two-frequency single-pass interferometry with a second receive antenna to generate DEMs over all land surfaces between -56º and +60º latitudes (Jordan et al., 1995; Werner, 1997). The accuracy of the released DEM generated by the US C-band radar interferometry should be in the order of the DTED level-1 accuracy (estimated to be around 10 m to 15 m). The accuracy of the DEM generated by the German X-band radar interferometry will be slightly better (estimated to be around 6 m to 10 m), but only for a partial coverage of the landmass. Will these products fulfil the requirements of all DEM users? The other satellite data resellers hope not, since many new satellites with high-resolution VIR or SAR sensors with along- or across-track stereo capability have been or are expected to be launched in the period 2000-2002 by US, Canadian, European, Indian, Russian, Japanese, etc., private or governmental organisations.

Acknowledgements

The authors would like to thank their CCRS friends Drs. Brian Brisco, Bert Guindon, Karim Mattar and Ridha Touzi and the anonymous external reviewer for the time they spent to review and improve this paper.

References

Bloom, A.L., E.J. Fielding, X.-Y. Fu, 1988. A demonstration of stereo-photogrammetry with combined SIR-B and Landsat-TM images. International Journal of Remote Sensing 9(5), 1023-1038.

Carlson, G.E., 1973. An improved single flight technique for radar stereo. IEEE Transactions on Geoscience Electronics GE-11(4), 199-204.

Curlander, J., 1982. Location of spaceborne SAR imagery. IEEE Transactions on Geoscience

and Remote Sensing 22(2), 106-112.

Domik, G., 1984. Evaluation of radar stereo viewability by means of simulation techniques. Proc. IGARSS'84, Paris, France, ESA-SP-215, 623-646.

Dowman, I.J., H. Ebner, C. Heipke, 1992. Overview of European developments in digital photogrammetric workstations. Photogrammetric Engineering and Remote Sensing 58(1), 51-56.

Dowman, I.J., Z.-G. Twu, P.H. Chen, 1997. DEM generation from stereoscopic SAR data. Proc. ISPRS Joint Workshop on Sensors and Mapping from Space, Hannover, Germany, September 29-October 2, 113-122.

Durden, S.L., J.J. van Zyl, H.A. Zebker, 1989. Modeling and observation of radar polarization signature of forested areas. IEEE Transactions on Geoscience and Remote Sensing 27(3), 290-301.

Ferretti, A., C. Prati, F. Rocca, 1999a. Multibaseline InSAR DEM reconstruction: The wavelet approach. IEEE Transactions on Geoscience and Remote Sensing 37(2), 705-715.

Ferretti, A., C. Prati, F. Rocca, 1999b. Permanent scatterers in SAR interferometry. Proc. IGARSS'99, Hamburg, Germany, June 28- July 2, 1528-1530.

Forster, R.R., K.C. Jezek, H. Gyoo Sohn, A.L. Gray, K.E. Mattar, 1998. Analysis of glacier flow dynamics from preliminary RADARSAT InSAR data of the Antarctic Mapping Mission. Proc. IGARSS'98, Seattle, USA, July 6-10, 2225-2227.

Frankot, T.R., R. Chellapa, 1988. A method for enforcing integrability in shape from shading. IEEE Transactions on Pattern Analysis and Machine Intelligence 10(4), 439-451.

Fullerton, J.K., F. Leberl, R.E. Marque, 1986. Opposite-side SAR image processing for stereo-viewing. Photogrammetric Engineering and Remote Sensing 52(9), 1487-1498.

Gabriel, A.K., R.M. Goldstein, 1988. Crossed-orbit interferometry: theory and experimental results from SIR-B. International Journal of Remote Sensing 9(5), 857-872.

Gabriel, A.K., R. Goldstein, H. Zebker, 1989. Mapping small elevation changes over large areas: differential radar interferometry. Journal of Geophysical Research 94(B7), 9183-9191.

Geudtner, D., P. Vachon, K.E. Mattar, A.L. Gray, 1997. RADARSAT repeat-pass SAR interferometry: results over an Arctic test site. Proc. GER'97 Symposium Geomatics in the Era of RADARSAT, Ottawa, Canada, May 25-30, CD-ROM.

Ghiglia, D.C, M.D. Pritt, 1998. Two-dimensional phase unwrapping: theory, algorithms and software. John Wiley & Sons, New York, USA, 493 p.

Goldstein, R., 1995. Atmospheric limitations to repeat-pass interferometry. Geophysical

Research Letters 22(18), 2517-2520.

Goldstein, R.M., H. Zebker, C. Werner, 1988. Satellite radar interferometry: two-dimensional phase unwrapping. Radio Science 23(4), 713-720.

Goldstein, R.M., H. Engelhardt, B. Kamb, R.M. Frolich, 1993. Satellite radar interferometry for monitoring ice sheet motion: application to an Antartic ice stream. Science 262(5139), 1525-1530.

Gracie, G., J.W. Bricker, R.K. Brewer, R.A. Johnson, 1970. Stereo radar analysis. Report FTR - 1339-1, U.S. Engineering Topography Laboratory, Fort Belvoir, VA, USA.

Gray, A.L., P.J. Farris-Manning, 1993. Repeat-pass interferometry with airborne synthetic aperture radar. IEEE Transactions on Geoscience and Remote Sensing 31(1), 180-191.

Gray, A.L., K.E. Mattar, P.W. Vachon, R. Bindschadler, K.C. Jezek, R. Forster, 1998. InSAR results from the RADARSAT Antarctic Mapping Mission data: estimation of glacier motion using a simple registration procedure. Proc. IGARSS'98, Seattle, USA, July 6-10, 1638-1640.

Guindon, B., 1990. Development of a shape-from-shading technique for the extraction of topographic models from individual spaceborne SAR images. IEEE Transactions on Geoscience and Remote Sensing 28(4), 654-661.

Hagberg, J.O., L.M.H. Ulander, J. Askne, 1995. Repeat-pass interferometry over forested terrain. IEEE Transactions on Geoscience and Remote Sensing 33(2), 331-340.

Horn, B., 1975. Obtaining shape from shading information. In. The Psychology of Computer Vision (Chapter 4), McGraw-Hill Book Company, New York, USA, pp. 115-155.

Jordan, R.L., B.L. Huneycutt, M. Werner, 1995. The SIR-C/X-SAR synthetic aperture radar. IEEE Transactions on Geoscience and Remote Sensing 33(4), 829-839.

Kaupp, V., L. Bridges, M. Pisaruk, H. MacDonald, W. Waite, 1983. Simulation of spaceborne stereo radar imagery: experimental results. IEEE Transactions on Geoscience and Remote Sensing 21(2), 400-405.

Kobrick, M., F. Leberl, J. Raggam, 1986. Radar stereo mapping with crossing flight lines. Canadian Journal of Remote Sensing 12(9), 132-148.

La Prade, G., 1963. An analytical and experimental study of stereo for radar. Photogrammetric Engineering 29(2), 294-300.

La Prade, G., E. Leonardo, 1969. Elevations from radar imagery. Photogrammetric Engineering 35(42), 366-371.

Leberl, F., 1972. On model formation with remote sensing imagery. Österreichische

Zeitschrift für Vermessungswesen 2, 43-61.

Leberl, F., 1979. Accuracy analysis of stereo side looking radar. Photogrammetric Engineering and Remote Sensing 45(8), 1083-1096.

Leberl, F., 1990. Radargrammetric image processing. Artech House, Norwood, USA, 595 p.

Leberl, F., G. Domik, J. Raggam, M. Kobrick, 1986a. Radar stereo-mapping techniques and applications to SIR-B images of Mount Shasta. IEEE Transactions on Geoscience and Remote Sensing 24(4), 473-481.

Leberl, F., G. Domik, J. Raggam, J. Cimino, M. Kobrick, 1986b. Multiple incidence angle SIR-B experiment over Argentina: stereo-radargrammetric analysis. IEEE Transactions on Geoscience and Remote Sensing 24(4), 482-491.

Leberl, F., K. Maurice, J.K. Thomas, M. Millot, 1994. Automated radar image matching experiment. ISPRS Journal of Photogrammetry and Remote Sensing 49(3), 19-33.

Li, F., R.M. Goldstein, 1990. Studies of multi-baseline spaceborne interferometric synthetic aperture radars. IEEE Transactions on Geoscience and Remote Sensing 28(1), 88-97.

Marr, D., T. Poggio, 1977. A computation of stereo disparity. Proc. Royal Society of London B194, 283-287.

Marr, D., E. Hildreth, 1980. A theory of edge detection. Proc. Royal Society of London B207, 187-217.

Massonnet, D., T. Rabaute, 1993. Radar inteferometry: limits and potential. IEEE Transactions on Geoscience and Remote Sensing 31(2), 455-464.

Massonnet, D., M. Rossi, C. Carmona, F. Adragana, G. Peltzer, K. Feigl, T. Rabaute, 1993. The displacement field of the Landers earthquake mapped by radar interferometry. Nature 364(6433), 138-142.

Massonnet, D., K. Feigl, 1995. Discrimination of geophysical phenomena in satellite interferograms. Geophysical Research Letters 22(12), 1537-1540.

Massonet, D., K. Feigl, 1998. Radar interferometry and its application to changes in the Earth's surface. Reviews of Geophysics 36(4), 441-500.

Mattar, K.E., AL. Gray, D. Geudtner, P. Vachon, 1999. Interferometry for DEM and terrain displacement: effects of inhomogeneous propagation. Canadian Journal of Remote Sensing 25(1), 60-69.

Moore, R.K., 1969. Heights from simultaneous radar and infrared. Photogrammetric Engineering 5(7), 649-651.

Paillou, Ph., M. Gelautz, 1999. Relief reconstruction from SAR stereo pairs: the "optimal gradient" matching method. IEEE Transactions on Geoscience and Remote Sensing 37(4),

2099-2107.

Paquerault, S., H. Maître, 1997. La radarclinométrie. Bullettin of the French Soc. of Photogr. and Rem. Sens. 148, 20-29.

Paquerault, S., H. Maître, 1998. A New Method for Backscatter Model Estimation and Elevation Map Computation Using Radarclinometry. Proc. EUROPTO - SPIE Conf. SAR Image Analysis, Modeling, and Techniques III, 23-24 September, Barcelona, Spain, Vol. 3497.

Parashar, S., E. Langham, J. McNally, S. Ahmed, 1993. RADARSAT mission requirements and concepts. Canadian Journal of Remote Sensing 18(4), 280-288.

Polidori, L., 1997. Cartographie radar. Gordon and Breach Science Publishers, Amsterdam, The Netherlands, 287 p.

Prati, C., F. Rocca, 1993.=Improving slant-range resolution with multiple SAR surveys. IEEE Transactions on Aerospace and Electronic Systems AES-29(1), 135-144.

Raggam, J., A. Almer, W. Hummelbrunner, D. Strobl, 1993. Investigation of the stereoscopic potential of ERS-1 SAR data. Proc. Fourth International Workshop on Image Rectification of Spaceborne Synthetic Aperture Radar, Loipesdorf, Austria, 26-28 May, 81-87.

Raggam, J., A. Almer, D. Strobl, 1994. A combination of SAR and optical line scanner imager for stereoscopic extraction of 3-D data. ISPRS Journal of Photogrammetry and Remote Sensing 49(4), 11-21.

Raggam, J., A. Almer, 1996 Assessment of the potential of JERS-1 for relief mapping Using optical and SAR data. International Archives of Photogrammetry and Remote Sensing, Vienna, Austria 31(B4), 671-676.

Ramapriyan, H., J. Strong, Y. Hung, C. Murray, 1986. Automated matching pairs of SIR-B images for elevation mapping. IEEE Transactions on Geoscience and Remote Sensing 24(4), 462-472.

Rosenfield, G.H., 1968. Stereo radar techniques. Photogrammetric Engineering 34, 586-594.

Schuler, D.L., J.S. Lee, K.W. Hoppel, 1993. Polarimetric SAR image signatures of the ocean and Gulf Stream features. IEEE Transactions on Geoscience and Remote Sensing 31(5), 1210-1221.

Schuler, D.L., J.S. Lee, G. De Grandi, 1996. Measurement of topography using polarimetric SAR images. IEEE Transactions on Geoscience and Remote Sensing 34(5), 1266-1277.

Schuler, D.L., T.L. Ainsworth, J.S. Lee, G.F. De Grandi, 1998. Topography mapping using polarimetric SAR data. International Journal of Remote Sensing 19(1), 141-160.

Simard, R., F. Plourde, Th. Toutin, 1986. Digital elevation modeling with stereo SIR-B image data. International Archives of Photogrammetry and Remote Sensing 26(7), 161-166.

Small, D., C. Werner, D. Nuesch, 1995. Geocoding of ERS-1 INSAR-derived digital elevation models. EARSeL Advances in Remote Sensing 4(2), 26-39 and I-II.

Sylvander, S., D. Cousson, P. Gigord, 1997. Étude des performances géométriques des images RADARSAT. Bulletin de la Société Française de Photogrammétrie et de Télédétection 148, 57-65.

Tarayre, H., D. Massonnet, 1996. Atmospheric propagation heterogeneities revealed by ERS-1 interferometry. Geophysical Research Letters 23(9), 989-992.

Thomas, J., W. Kober, F. Leberl, 1989. Multiple-image SAR shape from shading. Proc. IGARSS'89, Vancouver, Canada, July 10-14, 592-596.

Thomas, J., W. Kober, F. Leberl, 1991. Multiple-image SAR shape from shading. Photogrammetric Engineering and Remote Sensing 57(1), 51-59.

Toutin, Th., 1995. Generating DEM from stereo images with a photogrammetric approach: examples with VIR and SAR data. EARSeL Advances in Remote Sensing 4(2), 110-117.

Toutin, Th., 1996. Opposite-side ERS-1 SAR stereo mapping over rolling topography. IEEE Transactions on Geoscience and Remote Sensing 34(2), 543-549.

Toutin, Th., 1998. Evaluation de la précision géométrique des images de RADARSAT. Canadian Journal of Remote Sensing 24(1), 80-88.

Toutin, Th., 1999. Error tracking of radargrammetric DEM from RADARSAT images. IEEE Transactions on Geoscience and Remote Sensing 37(5), 2227-2238.

Toutin, Th., 2000a. Evaluation of radargrammetric DEM from RADARSAT images in high relief areas. IEEE Transactions on Geoscience and Remote Sensing 38(2), 782-789.

Toutin, Th., 2000b. Stereo-mapping with SPOT-P and ERS-1 SAR images. International Journal of Remote Sensing 21(8), 18p.

Toutin, Th., S. Amaral, 2000. Stereo RADARSAT data for canopy height in Brazilian forest. Canadian Journal for Remote Sensing 26(3), 189-200.

Touzi, R., A. Lopes, J. Bruniquel, P.W. Vachon, 1999. Coherence estimation for SAR imagery. IEEE Transactions on Geoscience and Remote Sensing 37(1), 135-149.

Ulaby, F.T., M.C. Dobson, 1988. Handbook on radar backscattering statistics for terrain. Artech House, 357 p.

Vachon, P., D. Geudtner, L. Gray, R. Touzi, 1995. ERS-1 synthetic aperture radar repeat-pass interferometry studies: Implications for RADARSAT. Canadian Journal of Remote Sensing 21(4), 441-454.

Valenzuela, G.R., 1968. Scattering of electromagnetic waves from a tilted slightly-rough surface. Radio Science 11(3), 1057-1066.

Wegmüller, U., Ch. Werner, 1995. SAR interferometric signature of forest. IEEE Transactions on Geoscience and Remote Sensing 33(2), 1153 – 1161.

Werner, M., 1997. Shuttle radar topography mission. Proc. of ISPRS Workshop: Sensors and Mapping from Space, Hannover, Germany, Sept. 29-Oct. 2, 9-11.

Wildey, R.L., 1984. Topography from single radar images. Sciences 224, 153-156.

Wildey, R.L., 1986. Radarclinometry for the Venus radar mapper. Photogrammetric Engineering and Remote Sensing 52(1), 41-50.

Yelizavetin, I.V., 1993. Digital terrain modeling from radar image stereopairs. Mapping Sciences and Remote Sensing 30(2), 151-160.

Yelizavetin, I.V., Y. A. Ksenofontov, 1996. Precision terrain measurement by SAR interferometry. Mapping Sciences and Remote Sensing 33(1), 1-19.

Yoritomo, K., 1972. Methods and instruments for the restitution of radar pictures. Proc. 12th ISP Congress, Ottawa, Canada, July 24-August 4. In, International Archives of Photogrammetry and Remote Sensing 20.

Zebker, H.A., J. Villasenor, 1992. Decorrelation in interferometric radar echoes. IEEE Transactions on Geoscience and Remote Sensing 30(5), 950-959.

Zebker, H.A., P.A. Rosen, R.A. Goldstein, C. Werner, A. Gabriel, 1994. On the derivation of coseismic displacement fields using differential radar interferometry. Journal of Geophysical Research-Solid Earth 99(10), 19617-19634.